



NRC Publications Archive Archives des publications du CNRC

Water permeation through catalyst-coated membranes

Adachi, Makoto; Romero, Tatiana; Navessin, Titichai; Xie, Zhong; Shi, Zhiqing; Mérida, Walter; Holdcroft, Steven

This publication could be one of several versions: author's original, accepted manuscript or the publisher's version. / La version de cette publication peut être l'une des suivantes : la version prépublication de l'auteur, la version acceptée du manuscrit ou la version de l'éditeur.

For the publisher's version, please access the DOI link below. / Pour consulter la version de l'éditeur, utilisez le lien DOI ci-dessous.

Publisher's version / Version de l'éditeur:

<https://doi.org/10.1149/1.3357339>

Electrochemical and Solid-State Letters, 13, 6, pp. B51-B54, 2010

NRC Publications Record / Notice d'Archives des publications de CNRC:

<https://nrc-publications.canada.ca/eng/view/object/?id=38de042b-4512-4f66-80c9-98816a8eac50>

<https://publications-cnrc.canada.ca/fra/voir/objet/?id=38de042b-4512-4f66-80c9-98816a8eac50>

Access and use of this website and the material on it are subject to the Terms and Conditions set forth at

<https://nrc-publications.canada.ca/eng/copyright>

READ THESE TERMS AND CONDITIONS CAREFULLY BEFORE USING THIS WEBSITE.

L'accès à ce site Web et l'utilisation de son contenu sont assujettis aux conditions présentées dans le site

<https://publications-cnrc.canada.ca/fra/droits>

LISEZ CES CONDITIONS ATTENTIVEMENT AVANT D'UTILISER CE SITE WEB.

Questions? Contact the NRC Publications Archive team at

PublicationsArchive-ArchivesPublications@nrc-cnrc.gc.ca. If you wish to email the authors directly, please see the first page of the publication for their contact information.

Vous avez des questions? Nous pouvons vous aider. Pour communiquer directement avec un auteur, consultez la première page de la revue dans laquelle son article a été publié afin de trouver ses coordonnées. Si vous n'arrivez pas à les repérer, communiquez avec nous à PublicationsArchive-ArchivesPublications@nrc-cnrc.gc.ca.





Water Permeation Through Catalyst-Coated Membranes

Makoto Adachi,^{a,b,*} Tatiana Romero,^{a,c} Titichai Navessin,^{a,z} Zhong Xie,^{a,**}
Zhiqing Shi,^a Walter Mérida,^{a,c,**} and Steven Holdcroft^{a,b,z}

^aInstitute for Fuel Cell Innovation, National Research Council Canada, Vancouver, British Columbia V6T 1W5, Canada

^bDepartment of Chemistry, Simon Fraser University, Burnaby, British Columbia V5A 1S6, Canada

^cClean Energy Research Centre, University of British Columbia, Vancouver, British Columbia V6T 1Z3, Canada

Water permeabilities, driven by concentration or pressure gradients, through NRE211 and catalyst-coated membranes are reported, and the effect of the catalyst layer (~18 μm thick, 30 wt % Nafion ionomer, carbon-supported Pt, 0.4 mg Pt cm⁻²) on membrane water permeation is deconvoluted. For the system studied, water permeation is limited by the bulk membrane; the effect of the catalyst layer was insignificant and, despite catalyst layers being deposited on the membrane's surface, it does not influence the rates of sorption or desorption at membrane interfaces.

© 2010 The Electrochemical Society. [DOI: 10.1149/1.3357339] All rights reserved.

Manuscript submitted December 23, 2009; revised manuscript received February 10, 2010. Published March 16, 2010.

During proton exchange membrane (PEM) fuel cell operation, water accumulates at the cathode due to both the electrochemical reduction of oxygen and electro-osmotic drag (EOD). An excess of water at the cathode may restrict oxygen from reaching catalytic reaction sites.¹⁻³ In contrast, the anode may suffer dehydration if the reactant gas is dry or if EOD is large, which leads to an increase in proton resistance.⁴⁻⁷ Except for very low current densities, the transport of protons and reactant gases collectively determine the current generated by a PEM fuel cell. Maintaining an adequate balance of water within an operating membrane electrode assembly is thus essential for its continuous operation. A preferential mode of water management is the transportation of water, accumulated at the cathode, to the anode.^{8,9}

Ex situ studies of water permeation through Nafion membranes reveal the importance of water vapor transport at the membrane interfaces.^{8,10-13} Water permeation through membranes exposed to liquid water on one side and nonsaturated vapor on the other is much larger than for membranes exposed to a differential water vapor pressure. Hydraulic pressure-driven water permeation, i.e., water permeation when the membrane is exposed to liquid water on both sides, is generally greater for membranes exposed to vapor on both sides, but smaller for membranes exposed to liquid water on one side and water vapor on the other.⁸

A catalyst layer (CL) comprises carbon-supported Pt particles and a proton-conducting ionomer. In the absence of freestanding CLs, experimental measurements of water permeation through CLs are difficult, and thus rely on theoretical and empirical models based on mass transport phenomena through porous media.^{1,14-18} The diffusivity of water vapor in CLs is reported to be a few orders of magnitude larger than in Nafion.^{13,19,29} However, because the sorption and desorption of water at the membrane interface significantly influence the permeability of the membrane to water, it is not unreasonable to conjecture that a CL might influence water sorption and desorption kinetics. For instance, hydrophilic nanopores in the CL may facilitate the condensation of water at the membrane surface due to a capillary effect,^{1,30} or the CL may change the area of the ionomer/water interface. The influence of CLs on the water permeability of membranes is the topic of this work. Water permeation is measured on freestanding membranes (NRE211), half-catalyst-coated membranes (hCCM_s) for which the CL is deposited on the water sorption side, half-catalyst-coated membranes (hCCM_d) for which the CL is deposited on the desorption side, and catalyst-coated membranes (CCMs) for which CLs are deposited on both sides. The acronyms and schematics of the samples are shown in

Fig. 1, together with a transmission electron microscopy (TEM) image of the PEM/CL interface, which shows the intimacy of contact between the two.

The following water permeation measurements were conducted:

1. Vapor-dry permeation (VDP), for which one side of the membrane is exposed to saturated water vapor, while dry helium gas is flowed over the other.^{10,11}
2. Liquid-dry permeation (LDP), for which one side of the membrane is exposed to liquid water and dry helium gas is flowed over the other.^{10,11}
3. Liquid-liquid permeation (LLP), for which both sides of the membrane are exposed to liquid water and water permeation is driven by a hydraulic pressure gradient.⁸

Experimental

Membranes and CCMs.—Nafion NRE211 membrane (25 μm, DuPont) was used as received. Freestanding membranes annealed for 6 h at 95°C on a vacuum table before use exhibited identical hydration and permeability characteristics as those of as-received membranes. A slurry of catalyst ink was prepared by dispersing carbon-supported Pt (46.5 wt % Pt, TEC10E50E, Tanaka Kikinokogyo) in 50:50 (vol %) methanol/water, followed by sonication for 30 min. A 5 wt% Nafion ionomer solution (EW1000, DuPont) was added so as to provide 30 wt % Nafion in the CL. The mixture was homogenized by sonication for 1 h. Catalyst ink was spray deposited using an automated spray coater (EFD, Nordson Co.) on both sides or on one side of the NRE211 membrane, mounted on a vacuum table heated to 95°C. The process was controlled to yield 0.35–0.40 mg cm⁻² of Pt on each side of the membrane. Further details are described in a previous article.³¹

Water permeability apparatus and experimental procedures.—**VDP and LDP.**—The setups illustrated in Fig. 2a and b were used for VDP and LDP measurements. Cylindrical chambers with volumes ~125 cm³ were separated by 2 cm² of membrane. Hot water was circulated through double-walled stainless steel chambers to control the cell temperature at 70°C. Dry helium gas was supplied to one chamber (dry side) and served as the carrier gas for the permeate water. The exhausts of both chambers were at ambient pressure. For VDP measurements, 25 mL min⁻¹ of dry nitrogen gas was bubbled through one of the chambers (wet side), which was half-filled with liquid water. This ensured a homogeneous distribution of saturated water vapor on the “wet side.” The setup for LDP measurements is shown in Fig. 2b. In this case, the wet side of the chamber was filled with liquid water so that the membrane was in direct contact with liquid water. In measurements of VDP and LDP, the dew point of the “dry side” was monitored while incrementally

* Electrochemical Society Student Member.

** Electrochemical Society Active Member.

^z E-mail: titichai.navessin@nrc-cnrc.gc.ca; holdcroft@sfu.ca

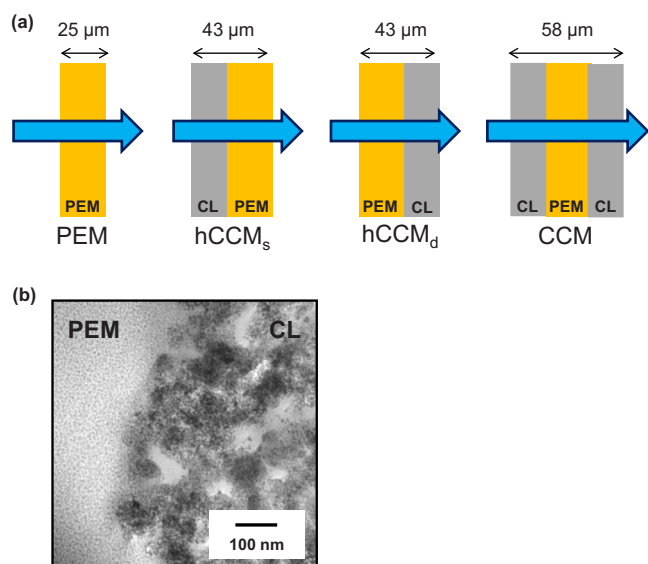
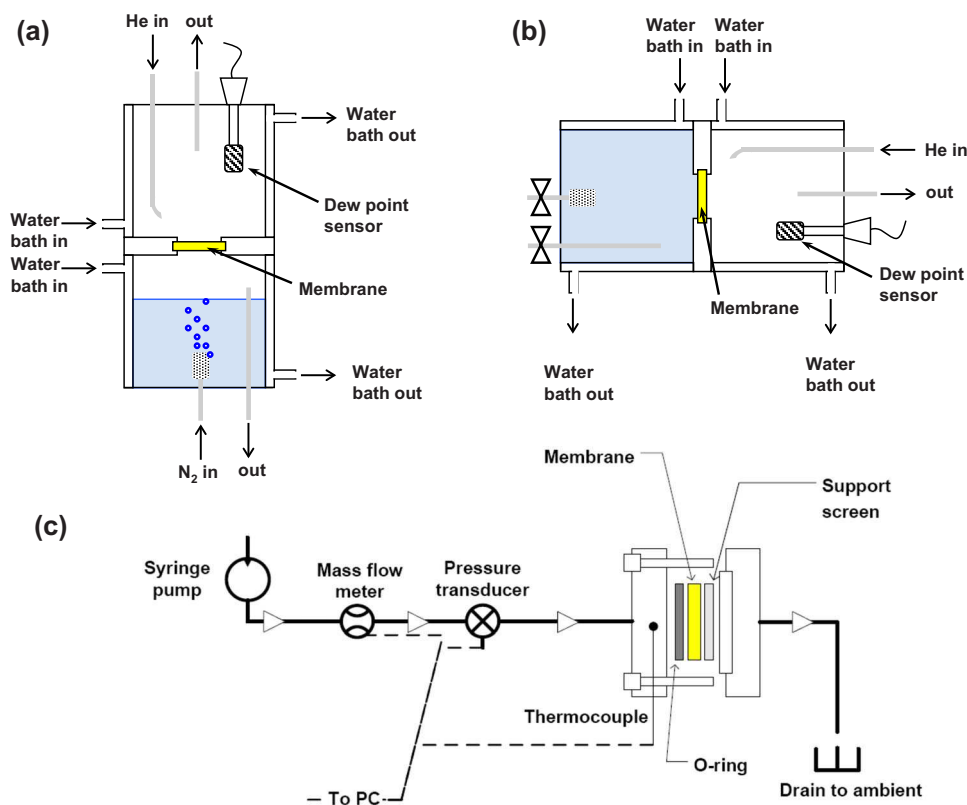


Figure 1. (Color online) (a) Schematic of the NRE211 and CCMs. PEM, pristine NRE211; hCCM_s (CL upstream of water permeation); hCCM_d (CL downstream of water permeation); CCM. (b) TEM image of the membrane/CL interface.

increasing the flow rate of the dry gas from 30 to 1000 mL min⁻¹. Further details of the measurements are described previously.^{10,11,32}

LLP.— Water permeation driven by a hydraulic pressure gradient (defined LLP) was measured using the setup illustrated in Fig. 2c. A syringe, mass flowmeter, and pressure transducer were connected in series. The cell was heated to 70°C. Further details of the measurement are found in a previous article.⁸



Results and Discussion

VDP.— VDP fluxes of water through the membrane and CCMs are plotted against the flow rate of the carrier gas in Fig. 3a. VDP fluxes increase with the flow rate, saturate, and gradually decrease at higher flow rates. For flow rates between 30 and 100 mL min⁻¹, the relative humidity (RH) of the dry side was estimated to be 25–10% according to the dew-point temperature. For higher flow rates, i.e., 300–1000 mL min⁻¹, the RH of the dry side was 4–1%. Increasing the flow rate reduces the RH on the dry side and increases the driving force for permeation across the membrane. The increase in the water permeation flux under a low flow rate (i.e., <100 mL min⁻¹) is due to an increase in the water concentration gradient across the membrane. In the high flow rate regime (300–700 mL min⁻¹), the reduced RH of the dry side may dehydrate the membrane interface and reduce the rate of water permeation.^{10–12} The intermediate flow rate range (i.e., 500–700 mL min⁻¹), within which fluxes are maximum, is representative of the relative rates of permeation in the absence of significant dehydration. Within all these flow rate regimes, no significant differences in water permeation were observed (<±10%) between NRE211 and CCMs. The presence of the CL does not affect the rate of permeation when deposited at the membranes' sorption or desorption interface or both.

LDP.— LDP fluxes of water through the membrane and CCMs increase with the increasing flow rate of the carrier gas, as shown in Fig. 3b. Similar to the case of VDP, this is due to the decreasing RH of the dry side, which increases the driving force for permeation. Because the LDP fluxes are 4–5 times larger than VDP, which is a consequence of having at least one liquid/membrane interface,^{10,12} severe dehydration of the membrane on the dry side is less likely. Thus, the flux did not reach a maximum within the flow rate studied. As with VDP measurements, the permeation fluxes through the NRE211 and CCMs were identical within the experimental error.

Figure 2. (Color online) Schematic diagrams of apparatus: (a) VDF,^{10,32} (b) LDP,^{10,32} and (c) LLP⁸ setups.

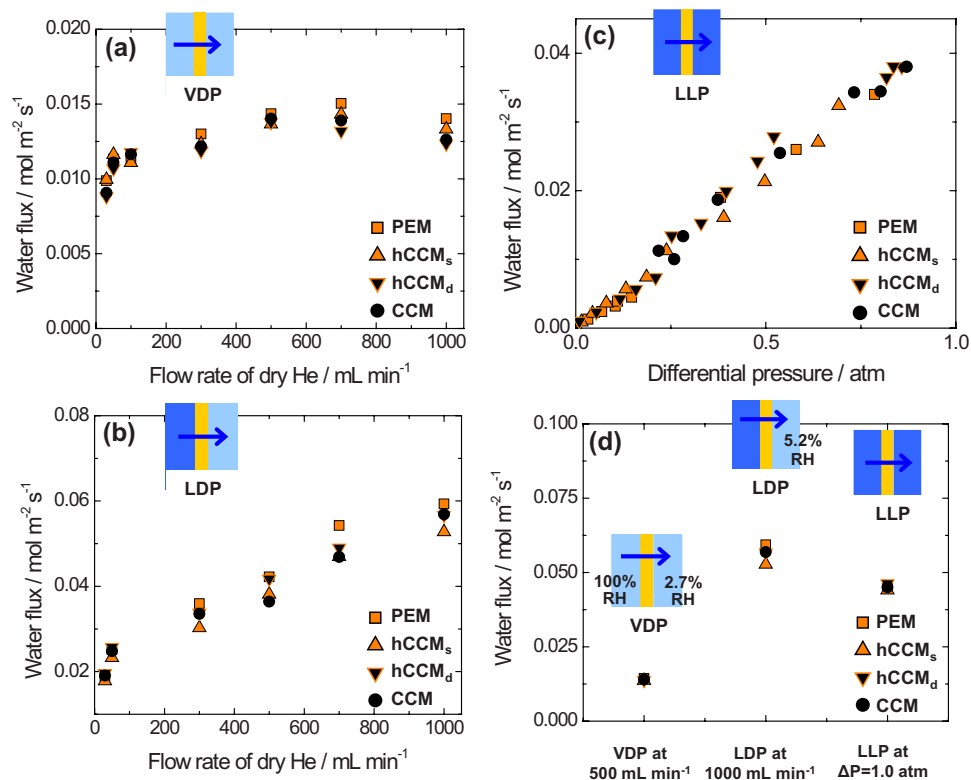


Figure 3. (Color online) Water permeation fluxes through NRE211 and CCMs at 70°C at (a) VDP and (b) LDP as a function of flow rate of the dry helium carrier gas, and (c) LLP as a function of differential hydraulic pressure. (d) Comparison of the representative water permeation fluxes measured by VDP, LDP, and LLP for the NRE211 and CCMs. All measurements were conducted at 70°C. PEM (□), hCCM_s (△), hCCM_d (▽), and CCM (●).

LLP.—The LLP flux of water increased linearly with applied pressure, as shown in Fig. 3c. The gradient of the slope represents the hydraulic permeance. These values are $(8.30 \pm 0.18) \times 10^{-12}$, $(8.02 \pm 0.14) \times 10^{-12}$, $(8.44 \pm 0.19) \times 10^{-12}$, and $(8.20 \pm 0.17) \times 10^{-12}$ m Pa⁻¹ s⁻¹ for PEM, hCCM_s, hCCM_d, and CCM, respectively, and are similar to the permeance values presented previously for NRE211.⁸ As with the VDP and LDP measurements, the presence of the CL had a negligible effect on the membrane's permeability to water.

Figure 3d compares water permeation fluxes through NRE211 and CCMs measured under VDP, LDP, and LLP conditions. Representative fluxes are taken at carrier gas flow rates of 500 and 1000 mL min⁻¹ and a differential pressure of 1.0 atm for VDP, LDP, and LLP, respectively. The RH values on either side of the membrane under various conditions are also provided in the figure. In this comparison, water fluxes associated with LDP and LLP are ~4 and ~3 times larger than fluxes measured under VDP conditions. This observation is consistent with previous studies for free-standing membranes.^{8,10,11} As intimated previously,⁸ this is due to the presence of liquid water at the membrane interface that maintains hydration and enhances water transport across the interface.

Conclusion

Three types of water permeation (VDP, LDP, and LLP) were measured for NRE211 and CCMs at 70°C. The difference in permeabilities of the NRE211 membrane (PEM), hCCM_s, hCCM_d, and CCM is negligible. The membrane is confirmed to be the “bottleneck” for water transport across CCMs; the presence of the CL apparently exerts no influence on the interfacial water sorption/desorption dynamics of the membrane interfaces, despite being located at the membrane/water interface. This is likely because the physical properties of the membrane extend into the CL.

Acknowledgment

The authors gratefully acknowledge financial support from the NRCC-National Hydrogen and Fuel Cell Program, Natural Sciences and Engineering Research Council of Canada, and the Consejo Na-

cional de Ciencia y Tecnología, Mexico. The authors thank Dr. Xinsheng Zhao, Dr. Michael Eikerling, Dr. Javier Gazzari, Dr. Jennifer Peron, and Tetsuya Mashio for fruitful discussions. The authors also thank the SFU machine shop for fabrication of the LLP cell.

Simon Fraser University assisted in meeting the publication costs of this article.

References

1. M. Eikerling, *J. Electrochem. Soc.*, **153**, E58 (2006).
2. M. K. Debe and A. J. Steinbach, *ECS Trans.*, **11**(1), 659 (2007).
3. J. M. L. Canut, R. M. Abouatallah, and D. A. Harrington, *J. Electrochem. Soc.*, **153**, A857 (2006).
4. Z. Shi and S. Holdcroft, *Macromolecules*, **38**, 4193 (2005).
5. J. Peron, A. Mani, X. Zhao, D. Edwards, M. Adachi, T. Soboleva, Z. Shi, Z. Xie, T. Navessin, and S. Holdcroft, *J. Membr. Sci.*, Submitted.
6. P. Berg, K. Promislow, J. St. Pierre, J. Stumper, and B. Wetton, *J. Electrochem. Soc.*, **151**, A341 (2004).
7. M. Eikerling, Y. Kharkats, A. A. Kornyshev, and Y. Volfkovich, *J. Electrochem. Soc.*, **145**, 2684 (1998).
8. M. Adachi, T. Navessin, Z. Xie, B. Frisken, and S. Holdcroft, *J. Electrochem. Soc.*, **156**, B782 (2009).
9. H. H. Voss, D. P. Wilkinson, P. G. Pickup, M. C. Johnson, and V. Basura, *Electrochim. Acta*, **40**, 321 (1995).
10. T. Romero and W. Mérida, *J. Membr. Sci.*, **338**, 135 (2009).
11. C. W. Monroe, T. Romero, W. Mérida, and M. Eikerling, *J. Membr. Sci.*, **324**, 1 (2008).
12. P. W. Majsztrik, M. W. Satterfield, A. B. Bocarsly, and J. B. Benzinger, *J. Membr. Sci.*, **301**, 93 (2007).
13. S. Ge, X. Li, B. Li, and I.-M. Hsing, *J. Electrochem. Soc.*, **152**, A1149 (2005).
14. Q. Wang, M. Eikerling, D. Song, and Z. S. Liu, *J. Electrochem. Soc.*, **154**, F95 (2007).
15. M. Secanell, K. Karan, A. Suleman, and N. Djilali, *Electrochim. Acta*, **52**, 22 (2007).
16. D. Song, Q. Wang, Z. Liu, T. Navessin, M. Eikerling, and S. Holdcroft, *J. Power Sources*, **126**, 104 (2004).
17. J. J. Baschuk and X. Li, *Appl. Energy*, **86**, 181 (2009).
18. J. J. Baschuk and X. Li, *J. Power Sources*, **86**, 181 (2000).
19. N. G. C. Astrath, J. Shen, D. Song, J. H. Rohling, F. B. G. Astrath, J. Zhou, T. Navessin, Z. S. Liu, C. E. Gu, and X. Zhao, *J. Phys. Chem. B*, **113**, 8369 (2009).
20. M. V. Williams, E. Begg, L. Bonville, H. R. Kunz, and J. M. Fenton, *J. Electrochem. Soc.*, **151**, A1173 (2004).
21. K. Sakai, K. Sato, T. Mashio, A. Ohma, K. Yamaguchi, and K. Shinohara, *ECS Trans.*, **25**(1), 1193 (2009).

22. K. Sato, A. Ohma, K. Yamaguchi, and K. Shinohara, *ECS Trans.*, **19**(17), 39 (2009).
23. K. Sato, A. Ohma, K. Yamaguchi, and K. Shinohara, *ECS Trans.*, **25**(1), 273 (2009).
24. X. Ye and C. Y. Wang, *J. Electrochem. Soc.*, **154**, B676 (2007).
25. X. Ye and C. Y. Wang, *J. Electrochem. Soc.*, **154**, B683 (2007).
26. T. Mashio, A. Ohma, and K. Shinohara, *ECS Trans.*, **16**(2), 1009 (2008).
27. T. Mashio, A. Ohma, S. Yamamoto, and K. Shinohara, *ECS Trans.*, **11**(1), 529 (2007).
28. T. A. Zawodzinski, M. Neeman, L. O. Sillerud, and S. Gottesfeld, *J. Phys. Chem.*, **95**, 6040 (1991).
29. S. Motupally, A. J. Becker, and J. W. Weidner, *J. Electrochem. Soc.*, **147**, 3171 (2000).
30. J. Liu and M. Eikerling, *Electrochim. Acta*, **53**, 13 (2008).
31. Z. Xie, X. Zhao, M. Adachi, Z. Shi, T. Mashio, A. Ohma, K. Shinohara, S. Holdcroft, and T. Navessin, *Energy Environ. Sci.*, **1**, 184 (2008).
32. T. Romero, Ph.D. Dissertation, University of British Columbia, Vancouver, BC, 2008).